

Homogenization of 2D materials in the Thomas–Fermi–von Weizsäcker theory

Saad Benjelloun,^{1,2} Salma Lahbabi,^{3,4} and Abdelqoddous Moussa⁴

¹⁾*De Vinci Higher Education, De Vinci Research Center, Paris, France*

²⁾*Makhbar Mathematical Sciences Research Institute, Casablanca, Morocco*

³⁾*Equipe de Mathématiques Appliquées, LARILE, ENSEM, Hassan II University of Casablanca, Morocco*

⁴⁾*College of Computing, Université Mohamed 6 Polytechnique, Benguerir, Morocco*

(*Electronic mail: abdelqoddous.moussa@um6p.ma)

(*Electronic mail: s.lahbabi@ensem.ac.ma)

(*Electronic mail: saad.benjelloun@devinci.fr)

(Dated: May 26, 2025)

We study the homogenization of the Thomas–Fermi–von Weizsäcker (TFW) model for 2D materials introduced in Ref. 6. It consists in considering 2D-periodic nuclear densities with periods going to zero. We study the behavior of the corresponding ground state electronic densities and ground state energies. The main result is that these three-dimensional problems converge to a limit model that is one dimensional, similar to the one proposed in Ref. 14. We also illustrate this convergence with numerical simulations and estimate the converging rate for the ground state electronic densities and the ground state energies.

Keywords: Thomas–Fermi–von Weizsäcker model, Homogenization, 2D materials, Periodic models, Crystals

CONTENTS

I. Introduction and main results	1
A. Thomas–Fermi–von Weizsäcker model for finite systems	2
B. Thomas–Fermi–von Weizsäcker model for 2D crystals	3
C. Homogenization of 2D materials	4
II. Hartree interaction	6
III. Homogenization procedure: proof of Theorem I.5	9
IV. Numerical illustration	14
References	15

I. INTRODUCTION AND MAIN RESULTS

In recent years, two-dimensional (2D) materials have become an intensely active research field, marked by landmark discoveries and widespread investigation^{11–13,15}, driven by their unique physical, electrical, chemical and optical properties, which significantly differ from their 3D counterparts¹⁶. Electronic structure simulations are highly useful in the discovery of these properties and their tuning for potential applications^{16,21,23}. Thus, the need for mathematical models and simulation algorithms tailored for 2D materials arises^{9,20,24}.

Density Functional Theory (DFT) is one of the most widely used simulation tools in electronic structure calculations. It consists of describing the electrons by their density ρ and the energy of the system by a functional of ρ . A famous model in this class is the (orbital free) Thomas–Fermi–von

Weizsäcker (TFW) model^{18,25}. From a mathematical point of view, an important result in the study of crystals is the thermodynamic limit problem. It consists of proving that when a finite cluster converges to some periodic perfect crystal, the corresponding ground state electronic density and ground state energy per unit volume converge to the periodic equivalent. This program has been carried out for the Thomas–Fermi–von Weizsäcker model for three-dimensional (3D) crystals in Ref. 10 and for one- and two-dimensional (1D and 2D) crystals in Ref. 6. Other properties of TFW-type models for crystals have been studied in the literature. The seminal work in Ref. 18 established the basic theory for atoms, molecules and crystals. Subsequent research addressed aspects such as the analysis of defects^{8,17}, stochastic materials⁵, potential symmetry breaking²², rigorous derivation of DFT models for 2D materials¹⁴, geometric optimisation⁴, and the emergence of periodic phenomena in large atoms³.

In this paper, we investigate the homogenization of the TFW model for 2D crystals. Our goal is to find a homogeneous material equivalent to a 2D crystal in the limit when the lattice parameter goes to zero. This corresponds to putting more and more (normalized) nuclei in the unit cell, or equivalently looking at the crystal from further and further away. It turns out that the homogenized material can be described by a 1D model, in the same spirit as in Ref. 14, which allows reducing computational time and resources required to simulate a 2D material, at least in a zero-order approximation. Our proof can be generalized if we substitute the $\int \rho^{5/3}$ term in the kinetic energy by $\int \rho^p$ for some $p > \frac{3}{2}$. Note that the strict convexity of the energy functional gives the uniqueness of the ground state, which plays an important role in the proof.

To our knowledge, the closest work to ours is Ref. 7 where the authors used the 2D TFW model⁶ to derive macroscopic features of a crystal from the microscopic structure in the presence of an external electric field. The crystal is modeled in the band $\mathbb{R}^2 \times [-1, 1]$ and micro–macro limit is taken when the ratio between the atomic spacing and the size of the crystal goes to zero.

The article is organized as follows. We start by recalling the Thomas–Fermi–von Weizsäcker model for finite systems in Section I A, and for 2D crystals in Section I B. In Section I C, we define the homogenization process, along with the limit problem, and state our main result, whose proof is detailed in Section III. Intermediate results about the 2D Coulomb interaction are presented in Section II. Finally, numerical illustrations are gathered in Section IV.

Acknowledgments The research leading to these results has received funding from OCP grant AS70 “Towards phosphorene-based materials and devices”. Prof. S. Lahbabi thanks the CERE-MADE for hosting her during the final writing of this article.

A. Thomas–Fermi–von Weizsäcker model for finite systems

We present in this section the TFW model for finite systems. Let $m \in L^1(\mathbb{R}^3, \mathbb{R}^+)$ be a finite nuclear charge density. The state of the electrons is described by a non-negative electronic density $\rho \in L^1(\mathbb{R}^3)$. The energy functional is given by

$$\mathcal{E}^m(\rho) = \int_{\mathbb{R}^3} |\nabla \sqrt{\rho}|^2 + \int_{\mathbb{R}^3} \rho^{5/3} + \frac{1}{2} D(\rho - m, \rho - m), \quad (1)$$

where the first two terms represent the kinetic energy of the electrons and $D(f, g)$ is the Coulomb interaction between charge densities f and g in the Coulomb space $\mathcal{C} = \left\{ f \in \mathcal{S}'(\mathbb{R}^3, \mathbb{R}), \widehat{f} \in L^2(\mathbb{R}^3) \right\}$. It is defined by

$$D(f, g) = \int_{\mathbb{R}^3} \int_{\mathbb{R}^3} \frac{f(x)g(y)}{|x-y|} dx dy = 4\pi \int_{\mathbb{R}^3} \frac{\widehat{f}(k)\widehat{g}(k)}{|k|^2} dk,$$

where $\widehat{f}(k)$ denotes the Fourier transform of f evaluated at k . The ground state is given by the following minimization problem

$$I^m = \inf \left\{ \mathcal{E}^m(\rho), \rho \geq 0, \sqrt{\rho} \in H^1(\mathbb{R}^3), \int_{\mathbb{R}^3} \rho = \int_{\mathbb{R}^3} m \right\}. \quad (2)$$

It is well known that problem (2) has a unique minimizer ρ (see for instance Ref. 2). $u = \sqrt{\rho}$ is the unique solution of the corresponding Euler–Lagrange equation

$$\begin{cases} -\Delta u + \frac{5}{3}u^{7/3} + u\Phi = \lambda u, \\ -\Delta\Phi = 4\pi(u^2 - m), \end{cases} \quad (3)$$

where $\lambda \in \mathbb{R}$, and $\Phi = (u^2 - m) * \frac{1}{|\cdot|}$ is the mean–field potential.

B. Thomas–Fermi–von Weizsäcker model for 2D crystals

We present in this section the TFW model for 2D crystals introduced in Ref. 6. 2D crystals are characterized by a nuclear density m that has the periodicity of a 2D lattice $\mathcal{R} = a_1\mathbb{Z} + a_2\mathbb{Z}$, where (a_1, a_2) are two linearly independent vectors in \mathbb{R}^2 (see Figure 1); namely

$$m(x_1 + k_1, x_2 + k_2, x_3) = m(x_1, x_2, x_3), \quad \forall x \in \mathbb{R}^3, \forall (k_1, k_2) \in \mathcal{R}.$$

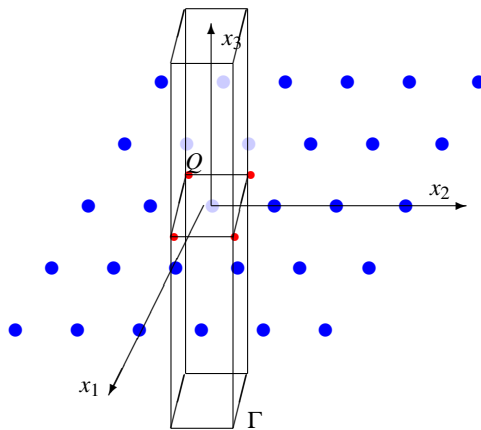


Figure 1. Example of a 2D lattice and its unit cell Γ .

From now on, we denote by Q the unit cell of $\mathcal{R} \subset \mathbb{R}^2$ and by $\Gamma = Q \times \mathbb{R}$ the unit cell of \mathcal{R} seen as a lattice in \mathbb{R}^3 . For $x \in \mathbb{R}^3$, we denote by $\underline{x} = (x_1, x_2) \in \mathbb{R}^2$ so that $x = (\underline{x}, x_3)$.

By means of a thermodynamic limit procedure, it has been shown in Ref. 6 that 2D crystals can be described by a model similar to (1)–(2) posed in the unit cell Γ . The main difference is that the 3D Green function $\frac{1}{|x|}$ is replaced by the 2D periodic Green function G solution of

$$-\Delta G = 4\pi \sum_{k \in \mathcal{R} \setminus \{0\}} \delta_k.$$

An explicit formula of G is given by Ref. 6, equation 11

$$G(x) = -\frac{2\pi}{|Q|} |x_3| + \sum_{k \in \mathcal{R}} \left(\frac{1}{|x - (k, 0)|} - \frac{1}{|Q|} \int_Q \frac{d\underline{y}}{|x - (\underline{y} + k, 0)|} \right). \quad (4)$$

It can be seen as the sum over the lattice of the Coulomb potential created by a point charge placed at the lattice sites, screened by a uniform background of negative unit charge. A Fourier decomposition of G can be found in Ref. 14. The 2D crystals energy functional then reads

$$\mathcal{E}_{\text{per}}^m(\rho) = \int_{\Gamma} |\nabla \sqrt{\rho}|^2 + \int_{\Gamma} \rho^{5/3} + \frac{1}{2} D_G(m - \rho, m - \rho), \quad (5)$$

where the Hartree interaction D_G is given by

$$D_G(f, g) := \int_{\Gamma} \int_{\Gamma} f(x)g(y)G(x-y) \, dx dy.$$

Remark I.1. In Ref. 6, there is a Coulomb correction term in the energy which comes from the Dirichlet boundary condition at infinity considered in the thermodynamic limit procedure, so that the energy is

$$\widetilde{\mathcal{E}}_{\text{per}}^m(\rho) = \mathcal{E}_{\text{per}}^m(\rho) + \frac{1}{|Q|} \int_{\Gamma} \int_{\Gamma} \frac{m(x)m(y)}{|x-y|}.$$

In our study, we omit this correction term as it does not affect the problem from a mathematical point of view.

The ground state is given by the minimization problem

$$I_{\text{per}}^m = \inf \left\{ \mathcal{E}_{\text{per}}^m(\rho), \quad \rho \geq 0, \quad \sqrt{\rho} \in X_{\text{per}}, \quad \int_{\Gamma} \rho = \int_{\Gamma} m \right\} \quad (6)$$

where

$$X_{\text{per}} = \left\{ v \in H_{\text{per}}^1(\Gamma), \quad (1 + |x_3|)^{1/2} v \in L_{\text{per}}^2(\Gamma) \right\}.$$

The weight $(1 + |x_3|)^{1/2}$ in the definition of the function space X_{per} is there to insure that $\rho := v^2$, with $v \in X_{\text{per}}$, satisfies $(1 + |x_3|)\rho \in L^1(\Gamma)$ and thus has a finite interaction energy, as the periodic potential G contains a term proportional to $|x_3|$. This problem has been studied in Ref. 6, section 3.2.3, along with some basic properties of the solution, that we summarize in the following Theorem.

Theorem I.2 (Ref. 6, Theorem 3.2). *Let $m \neq 0$ be a smooth non-negative, \mathcal{R} -periodic function with compact support w.r.t x_3 . Then, the minimization problem (6) has a unique minimizer ρ . Moreover, $u = \sqrt{\rho}$ is the unique solution of the corresponding Euler–Lagrange system*

$$\begin{cases} -\Delta u + \frac{5}{3}u^{7/3} + u\Phi = \lambda u, \\ -\Delta \Phi = 4\pi(u^2 - m), \end{cases} \quad (7)$$

where $\lambda \in \mathbb{R}$. In addition, $u \in L^\infty(\mathbb{R}^3)$ and $|u(x)| \leq \frac{C}{1 + |x_3|^{3/2}}$, for $|x_3| > 1$, $C > 0$ being a constant independent of the density m .

Remark I.3. *The fact that, in inequality $|u(x)| \leq \frac{C}{1 + |x_3|^{3/2}}$, for $|x_3| > 1$, the constant is independent of the density m , comes from a supersolution method applied to equation (7) (see Ref. 6, Theorem 3.1 and Theorem 2.3).*

C. Homogenization of 2D materials

In the framework of the Thomas–Fermi (TF) model and the reduced Hartree–Fock model (rHF), the recent work Ref. 14 studies reduced models for 2D homogeneous materials. The idea is that if the material is homogeneous, the 3D model is equivalent to a 1D model; simpler and less costly to simulate. In the present work, we are interested in the homogenization procedure, which models looking at a crystal macroscopically, from further and further away. Namely, we put more and more nuclei in the unit cell, with the right charge normalization, and we ask the following questions:

- What is the nuclear density at the limit?

- Does the ground state electronic density, potential and energy converge?
- What is the model describing the limit electronic structure?

Let m be a nuclear density satisfying the conditions of Theorem I.2 and consider the following sequence of nuclear densities which consists in putting N^2 small nuclei in the unit cell

$$m_N(x_1, x_2, x_3) := m(Nx_1, Nx_2, x_3), \quad \forall x \in \Gamma. \quad (8)$$

We note that m_N is $\frac{1}{N}\mathcal{R}$ -periodic, which describes a more homogeneous material than the initial one. The limit when $N \rightarrow +\infty$ describes a homogeneous material (see Figure 2). We will show that

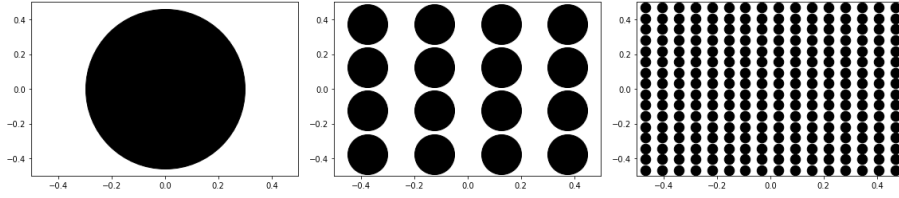


Figure 2. The homogenization process for the nuclear density m_N , illustrated at $N = 1, 4$ and 16 from left to right.

this model “converges”, in some sense that we will precise later, to the following limit model. For a 1D nuclear density μ , we introduce the energy functional

$$\mathcal{E}_1^\mu(\rho) = \int_{\mathbb{R}} |\nabla \sqrt{\rho}|^2 + \int_{\mathbb{R}} \rho^{5/3} + \frac{1}{2} D_1(\rho - \mu, \rho - \mu), \quad (9)$$

where the 1D Hartree interaction D_1 is defined for functions decaying fast enough by

$$D_1(f, g) = -2\pi \int_{\mathbb{R}} \int_{\mathbb{R}} |s - t| f(s) g(t) dt ds.$$

Here, the 1D Green kernel $-2\pi|t|$ is used. The ground state of this model is given by the minimization problem

$$I_1^\mu = \min\{E^\mu(\rho), \rho \geq 0, \sqrt{\rho} \in X_1, \int_{\mathbb{R}} \rho = \int_{\mathbb{R}} \mu\}, \quad (10)$$

where

$$X_1 = \left\{ v \in H^1(\mathbb{R}), (1 + |\cdot|)^{1/2} v \in L^2(\mathbb{R}) \right\}.$$

The following Theorem, which is a direct consequence of Theorem I.2 and the definitions of Hartree interaction terms D_G and D_1 , is similar to Ref. 14, Theorems 2.2 and 2.8, which treat Thomas–Fermi and reduced Hartree–Fock models.

Theorem I.4. *Let $\mu \in \mathcal{D}(\mathbb{R})$. The problem (10) has a unique minimizer. Moreover, $u := \sqrt{\rho}$ is the unique solution of the corresponding Euler–Lagrange equations*

$$\begin{cases} -u'' + \frac{5}{3}u^{7/3} + u\Phi = \lambda u, \\ -\Phi'' = 4\pi(u^2 - \mu), \end{cases}$$

where $\lambda \in \mathbb{R}$, and there exists $C > 0$, independent of μ , such that for any $|t| \geq 1$, $|u| \leq \frac{C}{1+|t|^{3/2}}$.

Our main contribution is the following Theorem.

Theorem I.5. *Let m be a nuclear density satisfying the hypothesis of Theorem I.2 and for $N \in \mathbb{N} \setminus \{0\}$, let m_N be defined as in (8). We denote by $I_N = I_{\text{per}}^{m_N}$ and by ρ_N the corresponding ground state given by Theorem I.2. Let $m_0(t) = \frac{1}{|\mathcal{Q}|} \int_{\mathcal{Q}} m(\underline{x}, t) d\underline{x}$ and denote by $I_0 = I_1^{m_0}$ and by ρ_0 the corresponding ground state given by Theorem I.4. The following holds*

- i. $\lim_{N \rightarrow \infty} I_N = I_0$,
- ii. ρ_N converges to ρ_0 in $L^1(\Gamma)$, in $L^p_{\text{loc}}(\Gamma)$ for all $1 \leq p \leq 3$, and almost everywhere,
- iii. $\sqrt{\rho_N}$ converges to $\sqrt{\rho_0}$ weakly in $H^1_{\text{per}}(\Gamma)$.

Our result is a zero order approximation of a finite N situation. In homogenization theory of partial differential equations with periodically oscillating coefficients, the two scale convergence technique is usually used to find higher order terms in the approximation¹. Applying a similar approach to our problem is a perspective of this work.

II. HARTREE INTERACTION

We recall in this section some properties of the Green function G , the Hartree interaction D_G and prove a uniqueness result of the mean field potential Φ . In the subsequent proposition, we introduce a convenient decomposition of the kernel G , which proves to be useful throughout the paper.

Proposition II.1. *We have*

$$G(x) = -\frac{2\pi}{|\mathcal{Q}|} |x_3| + \frac{1}{|x|} + \psi(x),$$

where $\psi \in L^\infty(\Gamma)$.

Proposition II.1 is partially proved in Ref. 6. We detail the proof here for consistency.

Proof. We start from the formula (4) of the explicit expression of the periodic Green function G

$$G(x) = -\frac{2\pi}{|\mathcal{Q}|} |x_3| + \sum_{\underline{k} \in \mathcal{R}} \left(\frac{1}{|x - (\underline{k}, 0)|} - \frac{1}{|\mathcal{Q}|} \int_{\mathcal{Q}} \frac{d\underline{y}}{|x - (\underline{y} + \underline{k}, 0)|} \right). \quad (11)$$

We then isolate the term corresponding to $\underline{k} = 0$ from the sum

$$\begin{aligned} G(x) = & -\frac{2\pi}{|\mathcal{Q}|} |x_3| + \left(\frac{1}{|x - (\underline{0}, 0)|} - \frac{1}{|\mathcal{Q}|} \int_{\mathcal{Q}} \frac{d\underline{y}}{|x - (\underline{y} + \underline{0}, 0)|} \right) \\ & + \sum_{\underline{k} \in \mathcal{R}^*} \left(\frac{1}{|x - (\underline{k}, 0)|} - \frac{1}{|\mathcal{Q}|} \int_{\mathcal{Q}} \frac{d\underline{y}}{|x - (\underline{y} + \underline{k}, 0)|} \right). \end{aligned}$$

We can thus rewrite G as

$$\begin{aligned} G(x) = & -\frac{2\pi}{|\mathcal{Q}|} |x_3| + \frac{1}{|x|} - \frac{1}{|\mathcal{Q}|} \int_{\mathcal{Q}} \frac{d\underline{y}}{|x - (\underline{y}, 0)|} \\ & + \sum_{\underline{k} \in \mathcal{R}^*} \left(\frac{1}{|x - (\underline{k}, 0)|} - \frac{1}{|\mathcal{Q}|} \int_{\mathcal{Q}} \frac{d\underline{y}}{|x - (\underline{y} + \underline{k}, 0)|} \right). \end{aligned}$$

Therefore we can write $G(x) = -\frac{2\pi}{|\mathcal{Q}|} |x_3| + \frac{1}{|x|} + \psi(x)$, where $\psi(x)$ is the sum of the remaining terms

$$\psi(x) = -\frac{1}{|\mathcal{Q}|} \int_{\mathcal{Q}} \frac{d\underline{y}}{|x - (\underline{y}, 0)|} + \sum_{\underline{k} \in \mathcal{R}^*} \left(\frac{1}{|x - (\underline{k}, 0)|} - \frac{1}{|\mathcal{Q}|} \int_{\mathcal{Q}} \frac{d\underline{y}}{|x - (\underline{y} + \underline{k}, 0)|} \right).$$

Let us show that $\psi \in L^\infty(\Gamma)$. The function $x \mapsto \frac{1}{|Q|} \int_Q \frac{d\underline{y}}{|x - (\underline{y}, 0)|}$ is continuous on Γ and goes to zero as $|x_3| \rightarrow \infty$. Moreover, the sum defining ψ converges normally on a neighborhood of $0_{\mathbb{R}^3}$ (see Ref. 6, Proposition 3.2). Therefore it is continuous on that neighborhood, which implies that ψ is bounded on $Q \times [-\varepsilon, \varepsilon]$, for some $\varepsilon > 0$. From Ref. 6, Equation 3.12, there exists $C > 0$ such that

$$\sum_{\underline{k} \in (\mathcal{A})^*} \left(\frac{1}{|x - (\underline{k}, 0)|} - \frac{1}{|Q|} \int_Q \frac{d\underline{y}}{|x - (\underline{y} + \underline{k}, 0)|} \right) \leq \frac{C}{|x_3|^\alpha}, \quad \forall \alpha < 1.$$

It follows that $x \mapsto \sum_{\underline{k} \in (\mathcal{A})^*} \left(\frac{1}{|x - (\underline{k}, 0)|} - \frac{1}{|Q|} \int_Q \frac{d\underline{y}}{|x - (\underline{y} + \underline{k}, 0)|} \right)$ is bounded on $x \in Q \times (\mathbb{R} \setminus [-\varepsilon, \varepsilon])$, thus ψ is also bounded on the same interval. \square

As a consequence of the above proposition, we prove useful properties of the potential Φ . Let us introduce some notations. For some domain $\Omega \subset \mathbb{R}^d$ and $1 \leq p \leq \infty$, we denote by

$$L_{\text{unif}}^p(\Omega) = \left\{ f \in L_{\text{loc}}^p(\Omega), \forall r > 0, \sup_{B(x,r) \subset \Omega} \|f\|_{L^p(B(x,r))} < \infty \right\},$$

where $B(x, r)$ is the ball of radius r centered at x . For $f \in L^p(\Gamma)$ and $g \in L_{\text{per}}^q(\Gamma)$, the convolution

$$(g *_{\Gamma} f)(x) = \int_{\Gamma} f(y)g(x-y) dy$$

is well-defined in $L_{\text{per}}^r(\Gamma)$, where $\frac{1}{p} + \frac{1}{q} = 1 + \frac{1}{r}$.

Proposition II.2. *Let*

$$Y_{\text{per}} = \left\{ f \in L^1(\Gamma) \cap L^{5/3}(\Gamma), \int_{\Gamma} f = 0, |\cdot| f \in L^1(\Gamma) \right\}.$$

The map

$$\begin{aligned} Y_{\text{per}} &\rightarrow L^\infty(\Gamma) \\ f &\mapsto G *_{\Gamma} f \end{aligned}$$

*is well-defined and continuous. Moreover, for $f \in Y_{\text{per}}$, $G *_{\Gamma} f$ is the unique solution, up to an additive constant, of the Poisson equation*

$$\begin{cases} \Phi \in L_{\text{unif}}^1(\mathbb{R}^3) \\ -\Delta \Phi = 4\pi f. \end{cases} \quad (12)$$

Proof. From Proposition II.1, we have $G(x) = \frac{1}{|x|} - \frac{2\pi}{|Q|} |x_3| + \psi(x)$, with $\psi \in L^\infty(\Gamma)$. We are thus going to bound the three functions

$$f *_{\Gamma} |x_3|, f *_{\Gamma} \frac{1}{|x|} \text{ and } f *_{\Gamma} \psi$$

in $L^\infty(\Gamma)$. First, since $\psi \in L^\infty(\Gamma)$, we have for any $x \in \Gamma$

$$\left| \int_{\Gamma} f(x-y) \psi(y) dy \right| \leq \|\psi\|_{L^\infty(\Gamma)} \|f\|_{L^1(x-\Gamma)}.$$

Thus

$$\|f *_{\Gamma} \psi\|_{L^\infty(\Gamma)} \leq \|\psi\|_{L^\infty(\Gamma)} \|f\|_{L^1(\Gamma)}.$$

We move to $f *_{\Gamma} \frac{1}{|x|}$. We have

$$\left| f *_{\Gamma} \frac{1}{|x|}(x) \right| \leq \int_{\Gamma} \frac{|f(x-y)|}{|y|} dy \leq \int_{\Gamma} |f(x-y)| dy + \int_{\Gamma} \frac{|f(x-y)|}{|y|} \mathbb{1}_{|y|<1} dy.$$

For the second term, we use Hölder inequality with $f \in L^{5/3}(\Gamma)$ and $\frac{1}{|y|} \mathbb{1}_{|y|<1} \in L^{5/2}(\Gamma)$. We conclude that

$$\left\| \frac{1}{|x|} *_{\Gamma} f \right\|_{L^{\infty}} \leq \|f\|_{L^1(\Gamma)} + \|f\|_{L^{5/3}(\Gamma)} \left\| \frac{1}{|y|} \mathbb{1}_{|y|<1} \right\|_{L^{5/2}(\Gamma)}.$$

Regarding the last term, we use the neutrality assumption to write

$$\int_{\Gamma} f(x-y) |y_3| dy = \int_{\Gamma} f(x-y) (|y_3| - |x_3|) dy.$$

Thus, using the triangle inequality and the \mathcal{B} -periodicity of $x \mapsto x_3 f(x)$, we obtain

$$\left| \int_{\Gamma} f(x-y) |y_3| dy \right| \leq \int_{\Gamma} |f(x-y)| |x_3 - y_3| dy = \int_{\Gamma} |f(y)| |y_3| dy.$$

We now prove that $G *_{\Gamma} f$ is the unique solution of (12). The function $G *_{\Gamma} f$ is \mathcal{B} -periodic, therefore it is bounded over \mathbb{R}^3 and also in $L^1_{\text{unif}}(\mathbb{R}^3)$. It satisfies equation (12) by the definition of G . Let Φ be another solution. Then $h = \Phi - G *_{\Gamma} f \in L^1_{\text{unif}}(\mathbb{R}^3)$ is a harmonic function over \mathbb{R}^3 . By the mean value Theorem for harmonic functions, we have that for any $x \in \mathbb{R}^3$,

$$h(x) = \frac{3}{4\pi} \int_{B(x,1)} h(y) dy.$$

Therefore,

$$|h(x)| \leq \frac{3}{4\pi} \sup_{z \in \mathbb{R}^3} \int_{B(z,1)} |h(y)| dy.$$

Since $h \in L^1_{\text{unif}}(\mathbb{R}^3)$, the supremum is finite, which implies h is bounded over \mathbb{R}^3 . By Liouville's Theorem, we conclude that h is constant. \square

Corollary II.3. *Let $f \in Y_{\text{per}}$, then $\nabla(G *_{\Gamma} f) \in (L^2(\Gamma))^3$ and there exists $C > 0$, such that*

$$D_G(f, f) = (4\pi)^{-1} \|\nabla(G *_{\Gamma} f)\|_{L^2(\Gamma)}^2 \leq C \|f\|_{L^1(\Gamma)} \left(\|f\|_{L^1(\Gamma)} + \|f\|_{L^{5/3}(\Gamma)} + \| |x| f \|_{L^1(\Gamma)} \right).$$

Proof. We have

$$D_G(f, f) = \int_{\Gamma} (G *_{\Gamma} f) \times f = -(4\pi)^{-1} \int_{\Gamma} (G *_{\Gamma} f) \times \Delta(G *_{\Gamma} f)$$

In Ref. 6, Section 3.2.1, it is shown using a hybrid Fourier transform, that is discrete in \underline{x} and continuous in x_3 , that

$$D_G(f, f) = \sum_{k \in \mathcal{R}} \int_{\mathbb{R}} \frac{|\widehat{f}(k, \xi)|^2}{\pi(|k|^2 + \xi^2)} d\xi.$$

Hence,

$$D_G(f, f) = (4\pi)^{-1} \sum_{k \in \mathcal{R}} \int_{\mathbb{R}} \left| \frac{(i2\pi(k, \xi)) \widehat{f}(k, \xi)}{\pi(|k|^2 + \xi^2)} \right|^2 d\xi = (4\pi)^{-1} \int_{\Gamma} |\nabla(\widehat{G *_{\Gamma} f})|^2 dx.$$

By the Planchrel-Parseval property⁶ of the hybrid Fourier transform, we conclude that

$$D_G(f, f) = (4\pi)^{-1} \int_{\Gamma} |\nabla(G *_{\Gamma} f)|^2.$$

Besides, by the previous proposition $G *_{\Gamma} f \in L^{\infty}(\Gamma)$ and

$$\|G *_{\Gamma} f\|_{L^{\infty}(\Gamma)} \leq (\|\psi\|_{L^{\infty}(\Gamma)} + 1) \|f\|_{L^1(\Gamma)} + \|f\|_{L^{5/3}(\Gamma)} \left\| \frac{1}{|y|} \mathbb{1}_{|y|<1} \right\|_{L^{5/2}(\Gamma)} + \|x|f\|_{L^1(\Gamma)} \leq C \|f\|_{Y_{\text{per}}},$$

which proves the inequality stated in the corollary. \square

III. HOMOGENIZATION PROCEDURE: PROOF OF THEOREM I.5

This section is devoted to the proof of Theorem I.5. The strategy of the proof is as follows. We start by proving the convergence of the nuclear densities $(m_N)_N$. Indeed, when N increases, the nuclear density m_N becomes more homogeneous and the sequence $(m_N)_N$ converges to the 2D homogeneous density $m_0(x_3) = \frac{1}{|Q|} \int_Q m(x) dx$ (see Lemma III.3). Electronic densities ρ_N are uniformly bounded w.r.t. N . We can thus extract convergent subsequences (see Proposition III.5). Both convergences give the upper bound $I_0 \leq \liminf I_N$. To prove the lower bound $I_0 \geq \limsup I_N$, we use ρ_0 as a test function. The proof is divided into four steps.

Step 1: Properties of the sequence $(m_N)_N$. We state below two properties of the sequence $(m_N)_N$.

Lemma III.1. *For $p \geq 1$ and $f \in L^1_{\text{loc}}(\mathbb{R})$ such that $x \mapsto f(x_3)m^p(x) \in L^1(\Gamma)$, we have*

$$\int_Q m_N^p(\underline{x}, x_3) d\underline{x} = \int_Q m^p(\underline{x}, x_3) d\underline{x}$$

and

$$\int_{\Gamma} f(x_3)m_N^p(x) dx = \int_{\Gamma} f(x_3)m^p(x) dx.$$

Proof. We have

$$\int_Q m_N^p(x_1, x_2, x_3) dx_1 dx_2 = \int_Q m^p(Nx_1, Nx_2, x_3) dx_1 dx_2 = \frac{1}{N^2} \int_{NQ} m^p(y_1, y_2, x_3) dy_1 dy_2.$$

As m is Q -periodic, then $\int_{NQ} m^p(y_1, y_2, x_3) dy_1 dy_2 = N^2 \int_Q m^p(y_1, y_2, x_3) dy_1 dy_2$. Hence, the first claim is proved. The second claim easily follows. \square

Remark III.2. *By the second point of Lemma III.1, with $f = 1$ and $p = 1$, we have that $\int_{\Gamma} m_N = \int_{\Gamma} m = \int_{\Gamma} m_0$, so that any admissible state for I_N is also an admissible state for I_0 , and vice versa.*

Lemma III.3. *The sequence $(m_N)_N$ converges to m_0 weakly in $L^p(\Gamma)$ for all $1 \leq p < +\infty$.*

Proof. From the Q -periodicity of m , we have for any $x_3 \in \mathbb{R}$ (see for instance Ref. 19)

$$m_N(\cdot, \cdot, x_3) \rightharpoonup m_0(x_3) \quad \text{in } L^p(Q), \quad \text{for all } 1 \leq p < \infty. \quad (13)$$

For $\varphi \in L^q(\Gamma)$, with $\frac{1}{q} + \frac{1}{p} = 1$, we have $f_N(x_3) := \int_Q m_N(x) \varphi(\underline{x}, x_3) d\underline{x} \rightarrow f(x_3) := m_0(x_3) \int_Q \varphi(\underline{x}, x_3) d\underline{x}$ a.e. and, by Hölder's inequality, we obtain

$$\begin{aligned}
|f_N(x_3)| &\leq \|\varphi(\cdot, \cdot, x_3)\|_{L^q(Q)} \left(\int_Q |m_N(\underline{x}, x_3)|^p d\underline{x} \right)^{1/p} \\
&= \|\varphi(\cdot, \cdot, x_3)\|_{L^q(Q)} \left(\int_Q |m(\underline{x}, x_3)|^p d\underline{x} \right)^{1/p} \in L^1(\mathbb{R}).
\end{aligned} \tag{14}$$

Thus, by the dominated convergence theorem,

$$\int_{\mathbb{R}} f_N(x_3) dx_3 = \int_{\Gamma} m_N(x) \varphi(\underline{x}, x_3) dx \rightarrow \int_{\mathbb{R}} f(x_3) dx_3 = \int_{\Gamma} m_0(x_3) \varphi(\underline{x}, x_3) dx.$$

□

Step 2: Convergence of electronic densities. The following proposition gives uniform bounds on quantities of interest w.r.t. N .

Proposition III.4. *There exist various constants C independent of N such that the following bounds hold.*

- i. $I_N \leq C$,
- ii. $\|\sqrt{\rho_N}\|_{H^1(\Gamma)} \leq C$,
- iii. $\|\rho_N\|_{L^p(\Gamma)} \leq C$ for all $1 \leq p \leq 3$,
- iv. $D_G(\rho_N - m_N, \rho_N - m_N) \leq C$.

Proof. As ρ_N is the minimizer of I_N and since m is an admissible test function for $\mathcal{E}_{\text{per}}^{m_N}$, we have

$$I_N = \mathcal{E}_{\text{per}}^{m_N}(\rho_N) \leq \mathcal{E}_{\text{per}}^{m_N}(m) = \int_{\Gamma} |\nabla \sqrt{m}|^2 + \int_{\Gamma} m^{5/3} + \frac{1}{2} D_G(m - m_N, m - m_N).$$

By Corollary II.3 applied to $f = m - m_N$ and Lemma III.1, we have

$$\begin{aligned}
D_G(m - m_N, m - m_N) &\leq C \|m - m_N\|_{L^1(\Gamma)} \left(\|m - m_N\|_{L^1(\Gamma)} + \|m - m_N\|_{L^{5/3}(\Gamma)} \right. \\
&\quad \left. + \||x|(m - m_N)\|_{L^1(\Gamma)} \right) \\
&\leq C \|m\|_{L^1(\Gamma)} \left(\|m\|_{L^1(\Gamma)} + \|m\|_{L^{5/3}(\Gamma)} + \||x|m\|_{L^1(\Gamma)} \right),
\end{aligned}$$

where, C denotes a generic positive constant that may differ from one line to the other. The finiteness of $\|\nabla \sqrt{m}\|_{L^2(\Gamma)}$, $\|m\|_{L^{5/3}(\Gamma)}$ and $\||x|m\|_{L^1(\Gamma)}$ follows directly from the assumed regularity and compact support of m in x_3 . Points ii–iv are easily deduced from point i. □

Proposition III.5. *There exists a non-negative function $\rho_0 \in L^1(\Gamma) \cap L^{5/3}(\Gamma)$ such that, up to a subsequence,*

- $(\rho_N)_N$ converges to ρ_0 strongly in $L^1(\Gamma)$ and $L_{\text{loc}}^p(\Gamma)$ for all $1 \leq p \leq 3$, weakly in $L^p(\Gamma)$, and almost everywhere on \mathbb{R}^3 ,
- $(\nabla \sqrt{\rho_N})$ converges to $\nabla \sqrt{\rho_0}$ weakly in $(L^2(\Gamma))^3$
- $\rho_0 - m_0 \in Y_{\text{per}}$
- The sequence $\nabla \Phi_N = \nabla(G *_{\Gamma}(\rho_N - m_N))$ converges to $\nabla \Phi_0 = \nabla(G *_{\Gamma}(\rho_0 - m_0))$ weakly in $(L^2(\Gamma))^3$.

As a consequence

$$\mathcal{E}_{\text{per}}^{m_0}(\rho_0) \leq \liminf I_N.$$

Proof. The sequence $(\sqrt{\rho_N})_N$ is uniformly bounded w.r.t. N in $H^1(\Gamma)$ by Proposition III.4. Then, up to a subsequence, it converges to some non-negative function u_0 weakly in $H^1(\Gamma)$, strongly in $L^p_{loc}(\Gamma)$ for all $2 \leq p \leq 6$ and almost everywhere on \mathbb{R}^3 . Besides, by Theorem I.2, there exists $C \geq 0$ such that for any N and any $x \in \mathbb{R}^3$ such that $|x_3| \geq 1$, it holds

$$|u_N(x)| \leq \frac{C}{1 + |x_3|^{3/2}}.$$

By the almost everywhere convergence, u_0 satisfies the same estimate, and we have for $\rho_0 := u_0^2$ the following estimate

$$|x_3| \rho_0(x) \leq \rho_0(x) 1_{|x_3| \leq 1} + \frac{C}{1 + |x_3|^3} \in L^1(\Gamma).$$

Thus $\rho_0 \in L^1(\Gamma) \cap L^{5/3}(\Gamma)$ and $|x_3| \rho_0 \in L^1(\Gamma)$.

We show now that ρ_N converges to ρ_0 strongly in $L^1(\Gamma)$. Let $\varepsilon > 0$ and R large enough such that for any $M, N \in \mathbb{N} \setminus \{0\}$

$$\int_{|x_3| > R} |\rho_N - \rho_M| \leq \frac{1}{R} \int_{|x_3| > R} |x_3| |\rho_N - \rho_M| \leq \frac{C}{R} \leq \frac{\varepsilon}{2}.$$

By the strong convergence of ρ_N in $L^1_{loc}(\Gamma)$, for M, N large enough, we have

$$\int_{|x_3| < R} |\rho_N - \rho_M| \leq \frac{\varepsilon}{2},$$

which proves that $(\rho_N)_N$ is a Cauchy sequence in $L^1(\Gamma)$. Besides, $(\nabla \Phi_N)_N$ is uniformly bounded in $L^2(\Gamma)$. Thus, it weakly converges, up to a subsequence, to $W \in (L^2(\Gamma))^3$. Since $-\Delta \Phi_N = 4\pi(\rho_N - m_N)$, then

$$\forall \varphi \in \mathcal{D}(\Gamma), \quad \int_{\Gamma} \nabla \Phi_N \cdot \nabla \varphi = 4\pi \int_{\Gamma} (\rho_N - m_N) \varphi. \quad (15)$$

By definition of the weak limit, the LHS of (15) converges to $\int_{\Gamma} W \cdot \nabla \varphi$, and since $\rho_N - m_N$ weakly converges to $\rho_0 - m_0$ in $L^1(\Gamma)$, then

$$\forall \varphi \in \mathcal{D}(\Gamma), \quad \int_{\Gamma} W \cdot \nabla \varphi = 4\pi \int_{\Gamma} (\rho_0 - m_0) \varphi.$$

Therefore $\operatorname{div} W = -4\pi(\rho_0 - m_0)$ in the sense of distributions. To conclude that $\int_{\Gamma} (\rho_0 - m_0) dx = 0$, we cannot directly apply the divergence theorem that needs the decay of W at $x = \pm\infty$, which is, a priori, only L^2 . Instead, we use the hybrid Fourier transform defined in Ref. 6, Eq. 3.13, and obtain, for \underline{R} in the dual lattice \mathcal{R}^* and $\eta \in \mathbb{R}$,

$$2i\pi \begin{pmatrix} R_1 \\ R_2 \\ \eta \end{pmatrix} \cdot \widehat{W}(R, \eta) = \widehat{(\rho_0 - m_0)}(R, \eta).$$

For $\underline{R} = 0$ and $\eta = 0$, we obtain $\int_{\Gamma} \rho_0 - m_0 = 0$. It follows that $\rho_0 - m_0 \in Y_{\text{per}}$. Thus by Proposition II.2, $\Phi_0 := G *_{\Gamma} (\rho_0 - m_0)$ is well-defined. Finally, we show that $\nabla \Phi_0 = W$. Let $\varphi = (\varphi_1, \varphi_2, \varphi_3) \in \mathcal{D}(\Gamma)^3$. We have $\operatorname{div} \varphi \in Y_{\text{per}}$, thus $G *_{\Gamma} (\operatorname{div} \varphi) \in L^{\infty}(\Gamma)$. Therefore

$$\begin{aligned} \langle \nabla G *_{\Gamma} (\rho_N - m_N), \varphi \rangle &= -\langle \rho_N - m_N, G *_{\Gamma} \operatorname{div} \varphi \rangle \\ &\rightarrow -\langle \rho_0 - m_0, G *_{\Gamma} \operatorname{div} \varphi \rangle = \langle \nabla G *_{\Gamma} (\rho_0 - m_0), \varphi \rangle. \end{aligned}$$

□

Step 3: Identification of the limit. We show next that ρ_0 is invariant w.r.t. (x_1, x_2) and it is indeed the unique minimizer of $\mathcal{E}_1^{m_0}$. This will prove that the convergences in Proposition III.5 hold for the whole sequence and prove points ii-iii of Theorem I.5.

We start by showing that ρ_0 is the unique minimizer of $\mathcal{E}_{\text{per}}^{m_0}$.

Proposition III.6. ρ_0 is the unique minimizer of $\mathcal{E}_{\text{per}}^{m_0}$.

Proof. Let $\rho \in \{\rho \geq 0, \sqrt{\rho} \in X_{\text{per}}, \int_{\Gamma} \rho = \int_{\Gamma} m_0\}$ be an admissible test function for $\mathcal{E}_{\text{per}}^{m_0}$. Let us show that

$$\mathcal{E}_{\text{per}}^{m_0}(\rho_0) \leq \mathcal{E}_{\text{per}}^{m_0}(\rho).$$

As $\int_{\Gamma} m_0 = \int_{\Gamma} m_N$ by Lemma III.1, ρ is also an admissible test function for $\mathcal{E}_{\text{per}}^{m_N}$. Thus

$$I_N = \mathcal{E}_{\text{per}}^{m_N}(\rho_N) \leq \mathcal{E}_{\text{per}}^{m_N}(\rho).$$

We know from Proposition III.5 that

$$\mathcal{E}_{\text{per}}^{m_0}(\rho_0) \leq \liminf I_N \leq \liminf \mathcal{E}_{\text{per}}^{m_N}(\rho).$$

It thus remains to show that $\mathcal{E}_{\text{per}}^{m_N}(\rho) \rightarrow \mathcal{E}_{\text{per}}^{m_0}(\rho)$, which boils down to showing that

$$D_G(\rho - m_N, \rho - m_N) \rightarrow D_G(\rho - m_0, \rho - m_0). \quad (16)$$

We recall that

$$D_G(f, g) = \int_{\Gamma \times \Gamma} f(x)f(y)G(x-y) \, dx \, dy,$$

with $G(x) = -2\pi|x_3| + \frac{1}{|x|} + \psi(x)$ and $\psi \in L^\infty(\Gamma)$. We denote by $h_N = \rho - m_N$ and $h = \rho - m_0$. We recall as well that for any $x_3 \in \mathbb{R}$, $h_N(\cdot, x_3)$ converges to $h(\cdot, x_3)$ weakly in $L^p(Q)$, for all $1 \leq p < \infty$. Therefore, for any $x_3, y_3 \in \mathbb{R}$, $h_N(\cdot, x_3)h_N(\cdot, y_3)$ converges to $h(\cdot, x_3)h(\cdot, y_3)$ weakly in $L^p(Q \times Q)$. We have $-2\pi|x_3 - y_3| + \psi(x-y) \in L^\infty(Q \times Q)$, and $\frac{1}{|x-y|} \in L^p(Q \times Q)$ for any $1 \leq p < 2$. Therefore, for any $x_3, y_3 \in \mathbb{R}$

$$\int_{Q \times Q} h_N(x)h_N(y)G(x-y) \, d\underline{x} \, d\underline{y} \rightarrow \int_{Q \times Q} h(x)h(y)G(x-y) \, d\underline{x} \, d\underline{y}. \quad (17)$$

To use a dominated convergence argument, we need to bound the LHS of (17) uniformly w.r.t. N by an L^1 function w.r.t. (x_3, y_3) . We start with the term with ψ . We have

$$\left| \int_{Q \times Q} h_N(x)h_N(y)\psi(x-y) \, d\underline{x} \, d\underline{y} \right| \leq \|\psi\|_{L^\infty(\Gamma)} \int_Q |h_N(x)| \, d\underline{x} \int_Q |h_N(y)| \, d\underline{y},$$

with

$$\int_Q |h_N| \, d\underline{x} \leq \int_Q \rho \, d\underline{x} + \int_Q m_N \, d\underline{x} = \int_Q \rho \, d\underline{x} + \int_Q m \, d\underline{x}. \quad (18)$$

The RHS of (18) is indeed an L^1 function w.r.t. to x_3 and y_3 . We move to the term with $|x_3|$. We have

$$\begin{aligned} \left| \int_{Q \times Q} h_N(x)h_N(y)|x_3 - y_3| \, d\underline{x} \, d\underline{y} \right| &\leq \int_Q |x_3 h_N(x)| \, d\underline{x} \int_Q |h_N(y)| \, d\underline{y} + \int_Q |y_3 h_N(y)| \, d\underline{y} \int_Q |h_N(x)| \, d\underline{x} \\ &\leq \left(\int_Q |x_3|(\rho(x) + m(x)) \, d\underline{x} \right) \left(\int_Q (\rho(y) + m(y)) \, d\underline{y} \right) \\ &\quad + \left(\int_Q |y_3|(\rho(y) + m(y)) \, d\underline{y} \right) \left(\int_Q (\rho(x) + m(x)) \, d\underline{x} \right). \quad (19) \end{aligned}$$

Again, the RHS of (19) is an L^1 function w.r.t. x_3 and y_3 . Finally, for the term with $\frac{1}{|x|}$, we split the term as follows

$$\begin{aligned} \int_{Q \times Q} h_N(x) h_N(y) \frac{1}{|x-y|} d\mathbf{x} d\mathbf{y} &= \int_{Q \times Q} \rho(x) (\rho(y) - 2m_N(y)) \frac{1}{|x-y|} d\mathbf{x} d\mathbf{y} \\ &\quad + \int_{Q \times Q} m_N(x) m_N(y) \frac{1}{|x-y|} d\mathbf{x} d\mathbf{y}. \end{aligned}$$

The first term is bounded by

$$\left| \int_{Q \times Q} \rho(x) (\rho(y) - 2m_N(y)) \frac{1}{|x-y|} d\mathbf{x} d\mathbf{y} \right| \leq \left\| \rho * \frac{1}{|x|} \right\|_{L^\infty(\Gamma)} \|\rho + 2m(\cdot, x_3)\|_{L^1(Q)},$$

which is an L^1 function w.r.t. x_3 . For the second term we use Young inequality with $p = q = r = 3/2$. We obtain

$$\begin{aligned} \left| \int_{Q \times Q} m_N(x) m_N(y) \frac{1}{|x-y|} d\mathbf{x} d\mathbf{y} \right| &\leq \|m_N(\cdot, x_3)\|_{L^{3/2}(Q)} \|m_N(\cdot, y_3)\|_{L^{3/2}(Q)} \left\| \frac{1}{|x|} \right\|_{L^{3/2}(Q)} \\ &\leq \|m(\cdot, x_3)\|_{L^{3/2}(Q)} \|m(\cdot, y_3)\|_{L^{3/2}(Q)} \times \left\| \frac{1}{|x|} \right\|_{L^{3/2}(Q)}. \end{aligned} \quad (20)$$

As m is compactly supported in x_3 , $x_3 \mapsto \|m(\cdot, x_3)\|_{L^{3/2}(Q)}$ is also compactly supported and it is an $L^{3/2}$ function, thus it is L^1 ; which concludes the proof. \square

Proposition III.7. *The density ρ_0 is invariant w.r.t. (x_1, x_2) , it is indeed the unique minimizer of the 1D model $\mathcal{E}_1^{m_0}$ and*

$$I_0 = \mathcal{E}_{\text{per}}^{m_0}(\rho_0) = \mathcal{E}_1^{m_0}(\rho_0).$$

Proof. For any $\underline{R} \in \mathbb{R}^2$, $\tau_{\underline{R}} \rho_0$ is also a minimizer of $\mathcal{E}_{\text{per}}^{m_0}$, where τ is the translation operator. Thus, by the convexity of the functional $\mathcal{E}_{\text{per}}^{m_0}$ and the uniqueness of its minimizer (see Theorem I.2), we deduce that ρ_0 is invariant w.r.t. (x_1, x_2) . To conclude the proof of the proposition, we notice that for any \mathbb{R}^2 -invariant function f

$$D_G(f, f) = D_1(f, f),$$

as shown in Ref. 14, Prop. 3.1. \square

Step 4: Convergence of the energy. We prove in this section point i of Theorem I.5, which consists of the convergence of the energy.

Proposition III.8. *We have*

$$I_0 = \lim I_N.$$

Proof. By Propositions III.5 and III.7, we have

$$I_0 \leq \liminf I_N.$$

To prove the lower bound on I_0 , we use ρ_0 as a test function for $\mathcal{E}_{\text{per}}^{m_N}$ and obtain

$$I_N \leq \int_{\Gamma} |\nabla \sqrt{\rho_0}|^2 + \int_{\Gamma} \rho_0^{5/3} + D_G(\rho_0 - m_N, \rho_0 - m_N) \rightarrow \mathcal{E}_{\text{per}}^{m_0}(\rho_0) = I_0,$$

where the last convergence is obtained using (16). Thus

$$\limsup I_N \leq I_0,$$

which concludes the proof of the proposition. \square

IV. NUMERICAL ILLUSTRATION

In this section, we illustrate the convergence result of Theorem I.5. We recall that the minimization problem (6) has a unique minimizer ρ and that $u := \sqrt{\rho}$ is the unique solution of the corresponding Euler–Lagrange equations

$$\begin{cases} \Delta u + \frac{5}{3}u^{\frac{7}{3}} + u\Phi = -\lambda u, \\ -\Delta\Phi = 4\pi(u^2 - \mu). \end{cases} \quad (21)$$

We numerically solve the 3D periodic Euler–Lagrange system in (21) by coupling a spectral approach and a fixed point iterative scheme (a python implementation can be accessed at https://github.com/sa3dben/TFW_model). We adopt the following iterative fixed point scheme: starting from an arbitrary initial guess u_0 , at each fixed point iteration, a linear eigenvalue problem is solved

$$\left(\Delta + \frac{5}{3}u_n^{4/3} + \Phi_n \right) u_{n+1} = -\lambda_1 u_{n+1}, \quad (22)$$

with Φ_n the solution to the Poisson equation $-\Delta\Phi_n = 4\pi(u_n^2 - \mu)$. The fixed point iterations are continued until convergence, i.e. $\|u_n - u_{n+1}\|_2 \leq \varepsilon$ for some tolerance $\varepsilon > 0$. We take $\varepsilon = 10^{-6}$ in our simulations.

We adopt a periodic setting, with the unit cell $\Gamma = Q \times [-\frac{L}{2}, \frac{L}{2}]$, and $Q = [-\frac{1}{2}, \frac{1}{2}]^2$. We use a Fourier series decomposition approach to solve the linearized equation (22). The solution is expected to be \mathcal{R} -periodic w.r.t. x_1 and x_2 and decaying at infinity w.r.t. $|x_3|$. Taking a large value for L , it is reasonable to impose period conditions in the third direction as well. Therefore, we consider the Fourier basis

$$f_k(x) = \frac{1}{\sqrt{L}} e^{i2\pi\left(x \cdot k + \frac{k_3 x_3}{L}\right)}.$$

We illustrate the convergence results in Theorem I.5 using the series of nuclei densities m_N defined as

$$m_N(x_1, x_2, x_3) = \mu(N, x_1) m_0(x_3) = \frac{5\pi}{2} |\cos(N\pi x_1)| \exp\left(-\frac{x_3^2}{8}\right).$$

We note that $\int_Q \mu(N, x_1) dx_1 dx_2 = \frac{\pi}{2} \int_Q |\cos(N \cdot \pi x_1)| = 1$. We take $L = 2\pi$, which proves effective as the function $m_0(x_3) = 5 \exp\left(-\frac{x_3^2}{8}\right)$ rapidly decreases in the x_3 direction. The same behaviour is assumed for the solutions u_N , and is validated with 1D simulations for (u_0, ρ_0) , the 1D solution corresponding to m_0 .

The different functions are sampled on a grid of dimensions $(200 \times N, 4, 300)$. We keep the discretization constant along the x_2 and x_3 -axis as the homogenization is only applied in the x_3 dimension. As we will only compute the zero Fourier mode along x_2 , four points are enough. We compute the positive Fourier modes up to indices $K = (K_1, K_2, K_3) = (4 \times N, 0, 6)$. On the x_3 -axis, we use the first 7 Fourier modes, found to be sufficient for accurate reconstruction of m_N and m_0 along that axis. Simulations in 1D prove that the solution $(u_0(x_3), \rho_0(x_3))$ is also accurately represented by these 7 modes. We assume that this is also the case in 3D for all values of N . The choice of $(4N + 1)$ Fourier modes in the x_1 direction, is motivated by the need for increased Fourier modes as N grows, to capture the changing characteristics and new harmonics for m_N and eventually for the solution (ρ_N, u_N) . In fact, we know that (ρ_N, u_N) will rather converge to a constant along the axis x_1 by Theorem I.5, however we enforce a hard check for this by computing also large modes for ρ_N and u_N .

Different L^p -norms of the error $e_N = \rho_N - \rho_0$ are presented in Figure 3 for values of $N = 1, \dots, 5$. We, indeed, observe the convergence stated in Theorem I.5. The same figure shows some convergence rates estimates. We conjecture that we have a theoretical convergence rate of $1/N^r$ with $\frac{10}{3} < r < 4$ for the different norms of e_N and the gradient L^2 norm $\|\nabla u_N - \nabla u_0\|_2$. The discrepancies in Figure 3 at $N = 4, 5$ are probably due to numerical errors.

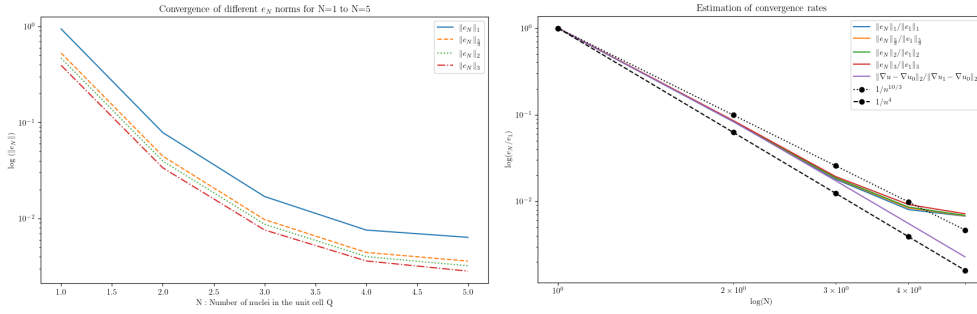


Figure 3. Convergence analysis for e_N norms (left) and convergence rates estimation for e_N norms and the gradient L^2 norm $\|\nabla u_N - \nabla u_0\|_2$ (right).

Figure 4 illustrates the convergence of the ground state energy $I_N = \mathcal{E}_{per}^{mN}(\rho_N)$ to the 1D energy $I_0 = \mathcal{E}_1^{m0}(\rho_0)$, proved in Theorem I.5. The estimated convergence rate for the energy is of the order $\approx \frac{1}{N^{3/2}}$.

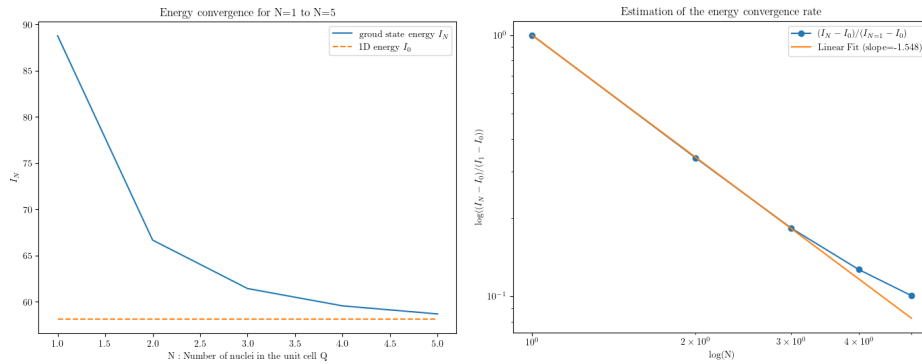


Figure 4. Convergence analysis for the energies I_N (left) and convergence rate estimation (right).

Remark IV.1. *It is noteworthy to mention that, for $N \geq 6$, and using higher order Fourier modes, the presence of numerical errors hinders a clear observation of further convergence for e_N .*

REFERENCES

- ¹G. ALLAIRE, *Homogenization and Two-Scale Convergence*, SIAM Journal on Mathematical Analysis, 23 (1992), pp. 1482–1518.
- ²R. D. BENGURIA, H. BREZIS, AND E. H. LIEB, *The Thomas–Fermi–von Weizsäcker Theory of Atoms and Molecules*, Communications in Mathematical Physics, 79 (1981), pp. 167–180.
- ³L. BJERG AND J. P. SOLOVEJ, *Periodicity of Atomic Structure in a Thomas–Fermi Mean-Field Model*. arXiv preprint arXiv:2406.19839 [math-ph], 2024.
- ⁴X. BLANC, *Geometry Optimization for Crystals in Thomas–Fermi Type Theories of Solids*, Communications in Partial Differential Equations, 26 (2001), pp. 651–696.
- ⁵X. BLANC, C. L. BRIS, AND P.-L. LIONS, *The energy of some microscopic stochastic lattices*, Archive for Rational Mechanics and Analysis, 184 (2007), pp. 303–339.
- ⁶X. BLANC AND C. LE BRIS, *Thomas–Fermi Type Theories for Polymers and Thin Films*, Advances in Differential Equations, 5 (2000), pp. 977–1032.
- ⁷X. BLANC AND R. MONNEAU, *Screening of an Applied Electric Field Inside a Metallic Layer Described by the Thomas–Fermi–von Weizsäcker Model*, Advances in Differential Equations, 7 (2002), pp. 847–876.
- ⁸E. CANCÈS AND V. EHRLACHER, *Local defects are always neutral in the thomas–fermi–von weizsäcker theory of crystals*, Archive for Rational Mechanics and Analysis, 202 (2011), pp. 933–973.

- ⁹A. CARVALHO, P. E. TREVISANUTTO, S. TAIOLI, AND A. H. CASTRO NETO, *Computational Methods for 2D Materials Modelling*, Reports on Progress in Physics, 84 (2021), p. 106501.
- ¹⁰I. CATTO, C. LE BRIS, AND P.-L. LIONS, *Mathematical Theory of Thermodynamic Limits: Thomas–Fermi Type Models*, Oxford University Press, 1998.
- ¹¹V. CHAUDHARY, P. NEUGEBAUER, O. MOUNKACHI, S. LAHBABI, AND A. EL FATIMY, *Phosphorene – An Emerging Two-Dimensional Material: Recent Advances in Synthesis, Functionalization, and Applications*, 2D Materials, 9 (2022), p. 032001.
- ¹²A. K. GEIM AND I. V. GRIGORIEVA, *Van der Waals Heterostructures*, Nature, 499 (2013), pp. 419–425.
- ¹³E. GERSTNER, *Nobel Prize 2010: Andre Geim and Konstantin Novoselov*, Nature Physics, 6 (2010), p. 836.
- ¹⁴D. GONTIER, S. LAHBABI, AND A. MAICHINE, *Density Functional Theory for Two-Dimensional Homogeneous Materials*, Communications in Mathematical Physics, 388 (2021), pp. 1475–1505.
- ¹⁵D. GUPTA, V. CHAUHAN, AND R. KUMAR, *A Comprehensive Review on Synthesis and Applications of Molybdenum Disulfide (MoS₂) Material: Past and Recent Developments*, Inorganic Chemistry Communications, 121 (2020), p. 108200.
- ¹⁶F. HUSSAIN, M. IMRAN, AND H. ULLAH, *Density Functional Theory (DFT) Study of Novel 2D and 3D Materials*, in Recent Trends in Nanomaterials: Synthesis and Properties, Springer Singapore, Singapore, 2017, pp. 269–284.
- ¹⁷A. KUMAR AND A. RAMABATHIRAN, *Analysis of Nearly Planar Defects Using the Thomas–Fermi–von Weizsäcker Model*. arXiv preprint arXiv:2408.11933 [math.AP], 2024.
- ¹⁸E. H. LIEB AND B. SIMON, *The Thomas–Fermi Theory of Atoms, Molecules and Solids*, Advances in Mathematics, 23 (1977), pp. 22–116.
- ¹⁹D. LUKKASSEN AND P. WALL, *On Weak Convergence of Locally Periodic Functions*, Journal of Nonlinear Mathematical Physics, 9 (2002), pp. 42–57.
- ²⁰A. PATRA, S. JANA, P. SAMAL, F. TRAN, L. KALANTARI, J. DOUMONT, AND P. BLAHA, *Efficient Band Structure Calculation of Two-Dimensional Materials from Semilocal Density Functionals*, The Journal of Physical Chemistry C, 125 (2021), pp. 11206–11215.
- ²¹K. REN, M. SUN, Y. LUO, S. WANG, J. YU, AND W. TANG, *First-Principle Study of Electronic and Optical Properties of Two-Dimensional Materials-Based Heterostructures Based on Transition Metal Dichalcogenides and Boron Phosphide*, Applied Surface Science, 476 (2019), pp. 70–75.
- ²²J. RICAUD, *Symmetry Breaking in the Periodic Thomas–Fermi–Dirac–von Weizsäcker Model*, Annales Henri Poincaré, 19 (2018), pp. 3129–3177.
- ²³Q. TANG, Z. ZHOU, AND Z. CHEN, *Innovation and Discovery of Graphene-like Materials via Density-Functional Theory Computations*, WIREs Comput Mol Sci, 5 (2015), pp. 360–379.
- ²⁴S. A. TAWFIK, O. ISAYEV, C. STAMPFL, J. SHAPTER, D. A. WINKLER, AND M. J. FORD, *Efficient Prediction of Structural and Electronic Properties of Hybrid 2D Materials Using Complementary DFT and Machine Learning Approaches*, Advanced Theory and Simulations, 2 (2019), p. 1800128.
- ²⁵C. F. VON WEIZSÄCKER, *Zur Theorie der Kernmassen*, Zeitschrift für Physik, 96 (1935), pp. 431–458.